Inorg. Chem. **2007**, *46*, 6245–6251

DNA Three-Way Junction with a Dinuclear Iron(II) Supramolecular Helicate at the Center: A NMR Structural Study

Leonardo Cerasino,[†] Michael J. Hannon,[‡] and Einar Sletten*[,†]

Department of Chemistry, University of Bergen, Allegt. 41, N-5007 Bergen, Norway, and School of Chemistry, The University of Birmingham, Edgbaston, Birmingham B15 2TT, U.K.

Received December 16, 2006

A tetracationic supramolecular helicate, $[Fe_2L_3]^{4+}$ ($L = C_{25}H_{20}N_4$), with a triple-helical architecture is found to induce the formation of a three-way junction (3WJ) of deoxyribonucleotides with the helicate located in the center of the junction. NMR spectroscopic studies of the interaction between the M enantiomer of the helicate and two different oligonucleotides, $[5'\text{-d(TATGGTACCATA)}]_2$ and $[5'\text{-d(CGTACG)}]_2$, show that, in each case, the 2-fold symmetry of the helicate is lifted, while the 3-fold symmetry around the helicate axis is retained. The 1:3 helicate/DNA stoichiometry estimated from 1D NMR spectra supports a molecular model of a three-way junction composed of three strands. Three separate double-helical arms of the three-way junction are chemically identical giving rise to one set of proton resonances. The NOE contacts between the helicate and DNA unambiguously show that the helicate is fitted into the center of the three-way junction experiencing a hydrophobic 3-fold symmetric environment. Close stacking interactions between the ligand phenyl groups and the nucleotide bases are demonstrated through unusually large downfield shifts (1–2 ppm) of the phenyl protons. The unprecedented 3WJ arrangement observed in solution has also been found to exist in the crystal structure of the helicate adduct of $[d(CGTACG)_2]$ (*Angew. Chem., Int. Ed.* **2006**, *45*, 1227).

Introduction

While the sequence of bases in DNA encodes the genetic information which defines features ranging from organism type through physical traits to disease susceptibility, the key to the expression of that information lies in recognition of the DNA structure and sequence. Thus, in nature, DNA information is processed and regulated by a plethora of DNA-binding proteins that form part of complex biological regulation and processing pathways.[2] The ability to stimulate or prevent the processing of the genetic code using artificial agents offers new opportunities not only for disease prevention or control but also to probe such pathways. Synthetic agents that recognize the genetic code are thus of great interest, particularly those that do so in some selective or specific fashion. Traditionally, this has meant sequence-specific recognition. However, this is not the only solution to this problem; rather, recognition of a particular unusual DNA structure may be a powerful alternative.

Small molecule agents that recognize DNA predominantly bind to DNA in one of four modes which were elucidated in the 1960s: alkylation/platination, intercalation, groove binding, and backbone binding. Alkylating agents form direct bonds to atoms on the DNA bases and include the clinical nitrogen mustard drugs, such as chlorambucil, and the very successful clinical platinum anti-cancer drugs, *cis*-platin, oxaliplatin, and carboplatin.[3] These agents tend to have a base-preference (e.g., GG for *cis*-platin) but to alkylate at many DNA sites, although attempts have been made to impart a sequence preference through conjugation to other DNA recognition motifs. Intercalators, such as doxorubicin,

* To whom correspondence should be addressed. E-mail: Einar.Sletten@kj.uib.no.
[†] University of Bergen.
[‡] The University of Birmingham.

(1) Oleksi, A.; Blanco, A. G.; Boer, R.; Usón, I.; Aymami, J.; Rodger, A.; Hannon, M. J.; Coll, M. *Angew. Chem., Int. Ed.* **2006**, *45*, 1227−1231.
(2) (a) Berg, J. M.; Tymoczko, J. L.; Stryer, L. *Biochemistry*, 5th ed.; Freeman: New York, 2002. (b) Branden, C.; Tooze, J. *Introduction to Protein Structure*, 2nd ed.; Garland: New York, 1999. (c) Neidle, S. *Nucleic Acid Structure and Function*; OUP: Oxford, U.K., 2002.
(3) (a) Lippert, B., Ed. *Cisplatin, Chemistry and Biochemistry of a Leading Anti-Cancer Drug*; Wiley-VCH: Weinheim, Germany, 1999. (b) Reedijk, J. *Chem. Commun.* **1996**, 801−806. (c) Guo, Z. J.; Sadler, P. J. *Adv. Inorg. Chem.* **2000**, *49*, 183−306. (d) Jamieson, E. R.; Lippard, S. J. *Chem. Rev.* **1999**, *99*, 2467−98. (e) Farrell, N. Inorganic Complexes as Drugs and Chemotherapeutic Agents. In *Comprehensive Coordination Chemistry, II*; McCleverty, J. A., Meyer, T. J.. Eds.; Elsevier Pergamon: Oxford, U.K., 2004; Vol. 9, pp 809−840 and references therein.

10.1021/ic062415c CCC: $37.00
Published on Web 04/04/2007

act by opening up the DNA and inserting between the base pairs[4] and have also found application in tumor treatment.[5] Although they may have a base preference they too bind at multiple sites. Minor groove recognition[6] by drugs such as the antiparasitic agent berenil offers greater scope for sequence selectivity, and some very elegant agents based on the natural antibiotic distamycin-A have been elaborated by Dervan.[7] Major groove binders also offer such possibilities although such recognition has been largely restricted to triplex formation by oligonucleotides and synthetic analogues[8] and peptide-recognition based on known biomolecular motifs.[9] Binding to the phosphate backbone is generally nonspecific.

We have been exploring the use of metallo-supramolecular agents to recognize DNA, reasoning that such large synthetic structures of dimensions similar to protein DNA recognition motifs would afford a more sizable recognition surface and lead to new effects. In particular, we have designed[10] and studied the DNA binding of a tetracationic triple-stranded helicate of ~2 nm length and ~1 nm diameter (similar dimensions to those of the α-helical DNA recognition unit of zinc fingers). This tetracationic helicate has been shown to bind strongly to ct-DNA as demonstrated by an ethidium bromide (EB) displacement assay which indicated binding constants well in excess of 10^7 M^{-1} at 20 mM NaCl. The helicate also induces unexpected and quite dramatic intramolecular DNA coiling, giving rise to small coils of DNA.[11]

Our initial studies included an NMR study of metallohelicate binding to a DNA oligonucleotide duplex, [d(GACGGCCGTC)$_2$].[12] However, because a racemic mixture of the helicate had to be used, the resulting 2D NMR spectra turned out to be quite complex preventing an unambiguous NMR structure determination. One model, obtained from the combination of NMR with molecular dynamics studies, was proposed where the helicate interacts at several sites in the major groove. This is consistent with the size of the agent, which is the right size and shape to bind in the DNA major groove and too large for the minor groove. Subsequent molecular dynamics simulations, which also reproduce the bending effects, have lent support to this as a binding mode.[13]

A method to obtain enantiomerically pure material has now enabled us to carry out NMR studies on adduct formation for the M and P enantiomers separately.[14] This greatly facilitates the analysis of the 2D NMR spectra of helicate/DNA adducts. Two different palindromic double-helical oligodeoxyribonucleotides containing a central, flexible TA-step, [d(TATGGTACCATA)]$_2$ (**1**) and [5′-d(CGTACG)]$_2$ (**2**), were chosen for these studies.

It was also decided that our co-workers in Barcelona led by Miquel Coll should carry out crystallographic work on the same duplexes in parallel to our NMR studies. They were subsequently able to obtain X-ray quality crystals of the M enantiomer in a complex with the hexanucleotide **2**.[1] The X-ray structure revealed not the helicate bound to a simple duplex but rather a DNA 3-way junction, in the heart of which resides the helicate in a trigonal hydrophobic cavity. Such a mode of DNA recognition is without precedent and has the potential to revolutionize how we think about molecules binding to DNA. It is particularly exciting as an alternative to strict sequence recognition for gaining specificity. While 3-way Y-shaped junction structures are much less well studied than 4-way X-shaped junctions, they are particularly intriguing because the DNA replication fork is a form of Y-shaped junction; 3-way junctions have also been found to be present in diseases such as Huntington's disease and myotonic dystrophy and in certain viral genomes.[15]

The observed formation of the 3-way junction (3WJ) in the X-ray structure is possible because in a palindromic sequence, Watson−Crick hydrogen bonding can be satisfied through a duplex structure, a 3-way junction, or higher-order junction structures (e.g., 4WJ, 5WJ, etc.).

The helicate had selected the 3-way junction from this dynamic combinatorial library of possibilities. The helicate and the junction appeared an almost perfectly matched pair, with neither significantly perturbed by binding. Nevertheless, we were conscious that the high symmetry frequently observed in crystal structures of large molecular assemblies is often dictated by the requirement of obtaining low packing energy, and the high-symmetry trigonal crystal structure (space group $P4_132$) of the 3WJ structure offered considerable packing energy.

The NMR studies reported herein describing the interaction between the helicate and the 6-mer and the 12-mer, respectively, confirm that the 3WJ structure is not merely a crystallographic artifact but a genuine structure that does prevail in solution. However, one should notice that a non-palindromic duplex does not have the ability to form a regular 3WJ. For such a system, groove binding could be an

(4) Lerman, L. S. *J. Mol. Biol.* **1961**, *3*, 18.
(5) Martínez, R.; Chacón-García, L. *Curr. Med. Chem.* **2005**, *12*, 127−151.
(6) Baraldi, P. G.; Bovero, A.; Fruttarolo, F.; Preti, D.; Tabrizi, M. A.; Pavani, M. G.; Romagnoli, R. *Med. Res. Rev.* **2004**, *24*, 475−528.
(7) Dervan, P. B. *Bioorg. Med. Chem.* **2001**, *9*, 2215−2235.
(8) (a) Da Ros, T.; Spalluto, G.; Prato, M.; Saison-Behmoaras, T.; Boutorine, A.; Cacciari, B. *Curr. Med. Chem.* **2005**, *12*, 71−88. (b) Thuong, N. T.; Helene, C. *Angew. Chem., Int. Ed. Engl.* **1993**, *32*, 666−690.
(9) Jantz, D.; Amann, B. T.; Gatto, G. J.; Berg, J. M. *Chem. Rev.* **2004**, *104*, 789−799 and references therein.
(10) Hannon, M. J.; Painting, C. L.; Hamblin, J.; Jackson, A.; Errington, W. *Chem. Commun.* **1997**, 1807−1808.
(11) (a) Hannon, M. J.; Moreno, V.; Prieto, M. J.; Moldrheim, E.; Sletten, E.; Meistermann, I.; Isaac, C. J.; Sanders, K. J.; Rodger, A. *Angew. Chem., Int. Ed.* **2001**, *40*, 880−884. (b) Meistermann, I.; Moreno, V.; Prieto, M. J.; Moldrheim, E.; Sletten, E.; Khalid, S.; Rodger, M.; Peberdy, J.; Isaac, C. J.; Rodger, A.; Hannon, M. J. *Proc. Natl. Acad. Sci. U.S.A.* **2002**, *99*, 5069−5074. (c) Uerpmann, C.; Malina, J.; Pascu, M.; Clarkson, G. J.; Moreno, V.; Rodger, A.; Grandas, A.; Hannon, M. J. *Chem.—Eur. J.* **2005**, *11*, 1750−1756.
(12) Moldrheim, E.; Hannon, M. J.; Meistermann, I.; Rodger, A.; Sletten, E. *J. Biol. Inorg. Chem.* **2002**, *7*, 770−780.
(13) Khalid, S.; Hannon, M. J.; Rodger, A.; Rodger, P. M. *Chem.—Eur. J.* **2006**, *12*, 3493−3506.
(14) Hannon, M. J.; Meisterman, I.; Isaac, C. J.; Blomme, C.; Aldrich-Wright, J.; Rodger, A. *Chem. Commun.* **2001**, 1078−1079.
(15) (a) Pearson, C. E.; Tam, M.; Wang, Y. H.; Montgomery, S. E.; Dar, A. C.; Cleary, J. D.; Nichol, K. *Nucleic Acids Res.* **2002**, *30*, 4534−47. (b) Sinden, R. R. *Nature* **2001**, *411*, 757−758. (c) Leonard, C. J.; Berns, K. I. *Prog. Nucleic Acid Res. Mol. Biol.* **1994**, *48*, 29−52. (d) Ren, J. S.; Qu, X. G.; Chaires, J. B.; Trempe, J. P.; Dignam, S. S.; Dignam, J. D. *Nucleic Acids Res.* **1999**, *27*, 1985−90. (e) Jensch, F.; Kemper, B. *EMBO J* **1986**, *5*, 181−189.

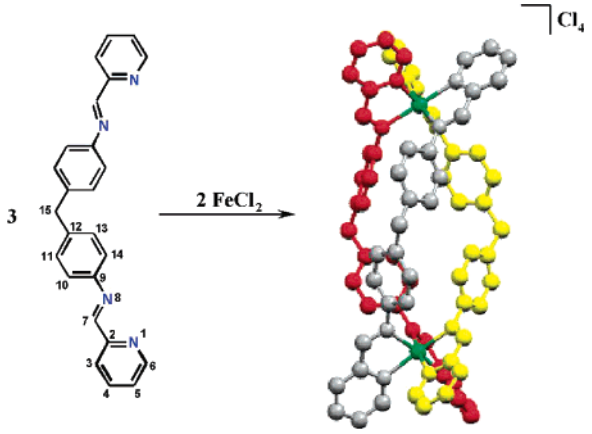

Figure 1. Molecular structure of the ligand (with numbering) and the tetracationic triple helical supramolecular helicate $[Fe_2(C_{25}H_{20}N_4)_3]Cl_4$.

Figure 2. Schematic drawing of the three-way junction.

alternative binding mode in accordance with theoretical calculations[13] and the CD-data on ct-DNA.[11b]

Materials and Methods

Starting Materials. The synthesis of $[Fe_2L_3]Cl_4$ ($L = C_{25}H_{20}N_4$) (Figure 1) has been described previously.[10] Enantiomerically pure material was obtained by using a cellulose (20 um, Aldrich) column.[11b] The 1D ^{1}H spectrum of the free helicate recorded at $T = 293$ K is shown in Figure 3. The sodium salts of the palindromic oligodeoxyribonucleotides, 5′-d(TATGGTACCATA) (**1**) and 5′-d(CGTACG) (**2**), were purchased from DNA Technology (Aarhus) and purified by HPLC on a C18 Waters X-terra column, desalted; paramagnetic impurities were removed using a Chelex 100 resin column (Sigma-Aldrich).

Sample Preparation. The oligonucleotides were dissolved in H_2O containing 10% D_2O, 10 mM phosphate buffer (pH 7.0), and 100 mM NaCl (final concentration ~1 mM in duplex). Aliquots of $[Fe_2L_3]Cl_4$ dissolved in CD_3OD (concentration = 10 mM) were added to the solution of oligonucleotides **1** and **2**. Titration was carried out until incipient precipitation was observed. At this stage, the amount of helicate added was ~1/3 of the starting oligonucleotide strand (on a molar basis). The sample was then freeze-dried to remove the methanol and redissolved in the desired solvent (either 90/10 H_2O/D_2O or just D_2O).

NMR Spectroscopy. ^{1}H NMR spectra were recorded on a Bruker DRY 600 MHz instrument at 293 K. A combination of through-space nuclear Overhauser effect (NOESY = nuclear Overhauser enhancement spectroscopy) at several mixing times (50, 200, and 800 ms) for **1** and only one mixing time (200 ms) for **2** were used. Through-bond-correlated two-dimensional spectra (TOCSY = total correlation spectroscopy) were recorded for both **1** and **2**. In addition, [^{31}P, H] HMBC experiments were recorded. For solutions containing 90/10 (H_2O/D_2O), double pulsed-field gradient spin-echo water suppression (dpfgsew5) was used.[16,17] The NMR data were processed using XWIN-NMR (Bruker) and analyzed using Sparky.[18]

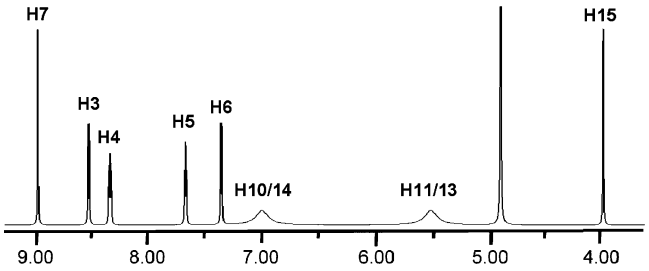

Figure 3. ^{1}H 1D NMR spectrum of $[Fe_2L_3]Cl_4$ in CD_3OD at 298 K.

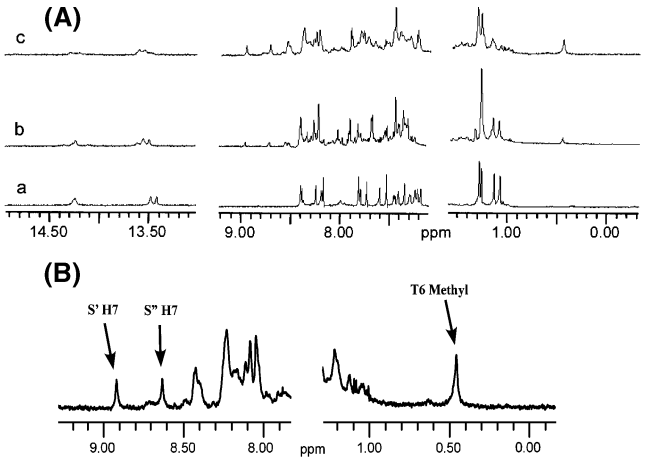

Figure 4. (A) ^{1}H NMR spectrum of $[Fe_2L_3]$/d($T_1A_2T_3G_4G_5T_6A_7C_8C_9A_{10}T_{11}A_{12}$)$]_2$ at 298 K at helicate/duplex ratios of (a) 0, (b) 0.25, and (c) 1. At the final concentration initial precipitation started to occur. (B) Expanded regions of ^{1}H 1D NMR spectrum of an aqueous solution containing $[Fe_2L_3]$-Cl_4/(TATGGTACCATA) at a 1:3 stoichiometric ratio.

Results and Discussion

The free Fe_2L_3 helicate is highly symmetric with a combined 3-fold and 2-fold symmetry giving six chemically equivalent subunits, each of which contains 10 protons. Complete assignment of all resonances is shown in Figure 3. The phenyl protons appear as two broadened resonances reflecting a restricted ring-spinning molecular motion. The ^{1}H NMR resonances of the free oligonucleotide [5′-d(TATGGTACCATA)]$_2$ have been assigned previously,[19] and analysis of DQF-COSY and short mixing-time NOESY spectra indicate that the duplex adopts a regular B-form DNA in aqueous solution at ionic strength of 0.1 M. A similar result was obtained for [5′-d(CGTACG)]$_2$ following the same assignment procedure.

Aliquots of the helicate solution were titrated into solutions of **1** and **2**, respectively, and the titration was monitored by 1D ^{1}H NMR. Figure 4a shows the proton spectra at different stages of titration, and in Figure 4b, an expansion of selected

(16) Liu, A. M.; Mao, X.; Ye, C.; Huang. H.; Nicholson, J. K.; Lindon, J. C. *J. Magn. Res.* **1998**, *132*, 125−129.
(17) Hwang, T-L.; Shaka, A. J. *J. Magn. Res., Ser. A* **1995**, *112*, 275−279.
(18) Goddard, T. D.; Kneller, D. G. *SPARKY3*; University of California: San Francisco, CA, DATE.
(19) Vinje, J.; Parkinson, J. A.; Sadler, P. J.; Brown, T.; Sletten, E. *Chem.—Eur. J.* **2003**, *9*, 1620−1630.

Table 1. ^{1}H Chemical Shifts (ppm) for $[5'\text{-d}(T_1A_2T_3G_4G_5T_6A_7C_8C_9A_{10}T_{11}A_{12})]_2$ **1** in the Adduct, Referenced to the HOD Signal at 4.764 ppm, 293 K[a]

	H8/H6	H2/H5/CH$_3$	H1′	H2′	H2″	H3′	H4′
T1	7.116	1.314	5.587	1.552	1.971	4.435	3.781
	−0.017	*−0.030*	*0.017*	*−0.039*	*−0.039*	*−0.015*	*0.008*
A2	8.267	7.638	6.121	2.647	2.791	4.801	4.225
	0.004	*0.042*	*−0.001*	*−0.007*	*0.002*	*−0.015*	*−0.004*
T3	7.002	1.199	5.529	1.835	2.198	4.609	3.963
	0.028	*0.016*	*0.018*	*0.006*	*−0.02*	*−0.039*	*−0.072*
G4	7.635		5.409	2.418	2.479	4.750	4.156
	0.033		*−0.099*	*−0.037*	*−0.01*	*−0.016*	*0.009*
G5	7.415		5.761	2.201	2.479	4.692	4.159
	0.016		*0.06*	*−0.077*	*−0.034*	*0.031*	*0.008*
T6	6.880	0.467	5.963	1.983	2.018	4.804	4.153
	−0.124	*−0.67*	*0.45*	*0.117*	*−0.252*	*0.152*	*0.204*
A7	8.029	7.505	5.070	2.206	2.429	4.577	3.921
	0.044	*0.347*	*−0.894*	*−0.247*	*−0.221*	*−0.217*	*−0.274*
C8	7.070	4.973	5.750	1.835	2.198	4.554	3.945
	0.017	*−0.019*	*0.177*	*0.046*	*0.009*	*0.011*	*−0.117*
C9	7.269	5.350	5.290	1.872	2.178	4.739	3.933
	0.043	*0.053*	*0.003*	*0.037*	*0.01*	*0.136*	*0.089*
A10	8.129	7.577	6.030	2.426	2.633	4.801	4.189
	0.034	*0.064*	*0.031*	*0.012*	*0.004*	*0.022*	*0.030*
T11	6.968	1.318	5.632	1.689	2.027	4.564	3.982
	0.032	*0.008*	*0.046*	*0.026*	*−0.007*	*−0.024*	*0.006*
A12	8.026	7.322	6.072	2.230	2.435	4.473	3.964
	0.027	*0.056*	*0.011*	*0.009*	*0*	*−0.011*	*0.083*

[a] The differences in chemical shifts between the free duplex and adduct are given in *italics*.

Table 2. ^{1}H Chemical Shifts for Nonexchangeable Protons of $[5'\text{-d}(C_1G_2T_3A_4C_5G_6)_2]$ in the Adduct, Referenced to the HOD Signal at 4.764 ppm at 290 K[a]

	H8/H6	H2/H5/CH$_3$	H1′	H2′	H2″	H3′	H4′
C1	7.666	5.921	5.712	2.000	2.421	4.656	4.015
	0.037	*0.032*	*−0.028*	*−0.015*	*0.009*	*−0.016*	*0.030*
G2	7.902		6.039	2.558	2.725	4.936	4.335
	−0.069		*0.091*	*−0.112*	*−0.036*	*−0.011*	*−0.002*
T3	7.153	0.796	6.229	2.238	2.238	4.990	4.349
	−0.123	*−0.705*	*0.591*	*0.125*	*−0.183*	*0.171*	*0.174*
A4	8.312	7.772	5.341	2.365	2.677	4.821	4.143
	0.020	*−0.003*	*−0.863*	*−0.319*	*−0.158*	*−0.181*	*−0.257*
C5	7.249	5.308	5.719	1.944	2.347	4.811	4.052
	−0.01	*−0.036*	*0.115*	*0.129*	*0.098*	*−0.043*	*−0.067*
G6	7.897		6.132	2.28	2.577	4.65	4.117
	0.026		*0.039*	*−0.025*	*0.029*	*0.034*	*−0.013*

[a] The differences in chemical shifts induced by adduct formation are given in *italics*.

regions is shown. Adduct formation induces specific changes in the proton spectrum of the supramolecular helicate and also in that of the oligonucleotides. Despite the fact that the spectrum is very crowded, especially in the aromatic region where resonances from both aromatic nucleobases and helicate protons overlap, a few key resonances are identified. First, the resonance corresponding to the helicate imine proton (H7), which lies in a noncrowded region of the 1D spectrum, is split into two clearly resolved peaks with chemical shift changes of 0.12 and −0.20 ppm, respectively. The corresponding imine chemical shift changes observed for **2** are 0.10 and −0.10 ppm, respectively (data not shown). For both **1** and **2**, the two new H7 signals have equal intensity from the beginning of the titration until the end, confirming that both signals belong to the bound helicate rather than originating from two different helicate species (i.e., bound and unbound). Each helicate contains 6 imine protons. The fact that the 1D spectrum of the adduct shows only two separate imine signals of equal intensity means that the 2-fold symmetry, but not the 3-fold symmetry, of the helicate is lifted in the bound species.

Second, the methyl signal corresponding to the methyl group of the central thymine residue in **1** and **2** experiences a large and almost equal upfield chemical shift change: −0.67 ppm for **1** and −0.70 ppm for **2** (Tables 1 and 2). A comparison of the integrated intensity of the central methyl signal with that of the helicate imine signal gives a helicate to DNA single-strand ratio of approximately 1:3. These observations indicate that the complexed species contains one helicate for every three oligonucleotide strands. Because the helicate retains its 3-fold symmetry, the oligonucleotide strands represent a 3-fold symmetric environment. Furthermore, the presence of identical oligonucleotide strands excludes the possibility that the helicate is bound in a groove of a triple-helical DNA structure.

Tables 1−3 present the chemical shifts for the nonexchangeable protons of adduct **1** and **2**. The chemical shift variation for DNA protons H6/H8, H1′, H2′/2″, and H3′ along the chain are represented graphically in Figure 5. It is evident that a large number of the nucleobases retain their native duplex geometry. Two separate pathways, S′ and S″ could be traced for the helicate proton resonances in the NOESY map. As inferred from the 1:1 ratio in the 1D spectrum, the two pathways correspond to the two ends of the helicate merging at the methylene bridge where cross-peaks are observed between H15′ and H15″ and between each of them and H11′ and H11″. This is clear evidence that both sets stem from the same bridging ligand which has lost its 2-fold symmetry. The phenyl bridges of the helicate undergo internal rotation in the unbound state resulting in broad composite H10/14 and H11/13 signals at room temperature (Figure 3). However, in the adduct, the internal rotation is hindered resulting in separate sharp signals for each of the phenyl protons. Moreover, these protons are shown to experience large chemical shift changes in the range of 0.2−2.3 ppm (see Table 3). The dramatic chemical shift changes of the phenyl and methylene resonances induced by the oligonucleotide environment would be consistent with this area of the helicate being engaged in strong π-stacking interactions with the purine or pyrimidine rings.

At first it was quite surprising to observe that only proton resonances representing the central TA residues experienced significant chemical shifts as shown in Figure 5. The facts that only the central part of the duplex was perturbed and that the helicate apparently is located in a 3-fold symmetric environment pointed toward an unusual molecular arrangement. At this stage, it was important to verify that Watson−Crick base pairing was retained. The 1D spectrum of the imino region recorded for **1** exhibits extremely broad peaks making it difficult to assign the imino protons involved in hydrogen bonding. However, the 2D map shown in Figure 6 gives clear evidence that the eight central base pairs are intact. The NOESY imino region shows cross-peaks between the imino−amino protons of the two GC base-pairs and between the imino−A-H2 proton of the central TA base-

Table 3. ^{1}H Chemical Shifts (ppm), (293 K), for $[Fe_2L_3]^{4+}$ for Adduct **1** and Adduct **2**

	adduct **1**										
	H7	H3	H4	H5	H6	H10	H11	H13	H14	H15′	H15″
S′	8.93	8.42	8.22	7.51	7.16	5.07	6.27	3.64	4.70		
	0.12	*0.05*	*0.04*	*0.00*	*0.02*	*−1.76*	*0.95*	*−1.69*	*−2.13*	2.29	2.39
	8.62	8.37	8.16	7.43	7.07	5.10	6.40	4.05	5.29	*−1.51*	*−1.41*
S″	*−0.20*	*0.00*	*−0.02*	*−0.08*	*−0.10*	*−1.07*	*1.08*	*−1.28*	*−1.54*		
	adduct 2										
	H7	H3	H4	H5	H6	H10	H11	H13	H14	H15′	H15″
S′	9.09	8.61	8.40	7.70	7.34	5.30	6.50	3.89	5.57		
	0.10	*0.07*	*0.05*	*0.02*	*−0.01*	*−1.70*	*1.00*	*−1.61*	*−1.43*	2.55	2.69
S″	8.89	8.63	8.38	7.66	7.31	5.36	6.69	4.30	5.56	*−1.42*	*−1.28*
	−0.10	*0.09*	*0.03*	*−0.02*	*−0.04*	*−1.64*	*1.19*	*−1.20*	*−1.44*		

[a] The differences in chemical shifts between the adduct and the free helicate are given in *italics*.

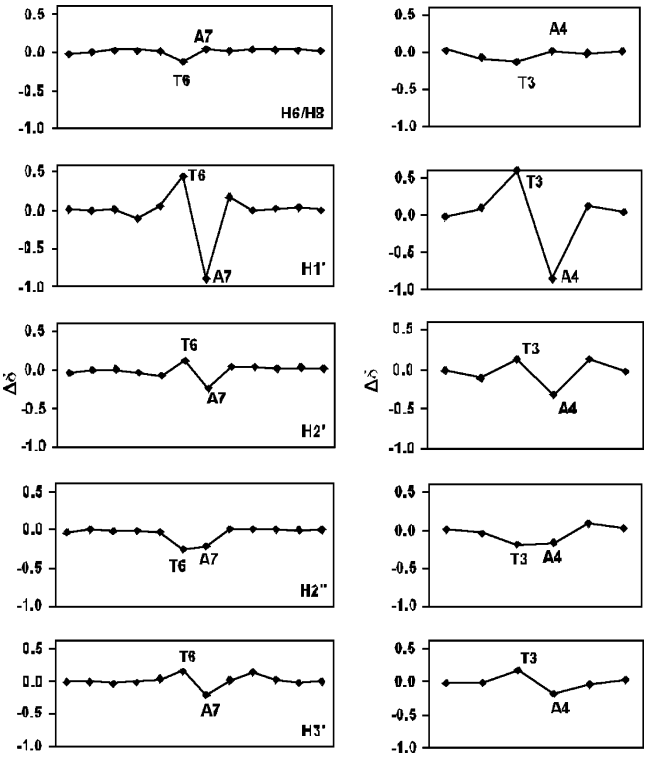

Figure 5. Helicate-induced ^{1}H NMR chemical shift differences of selected protons of (a) $[d(TATGGTACCATA)]_2$ and (b) $[5'\text{-}d(CGTACG)]_2$.

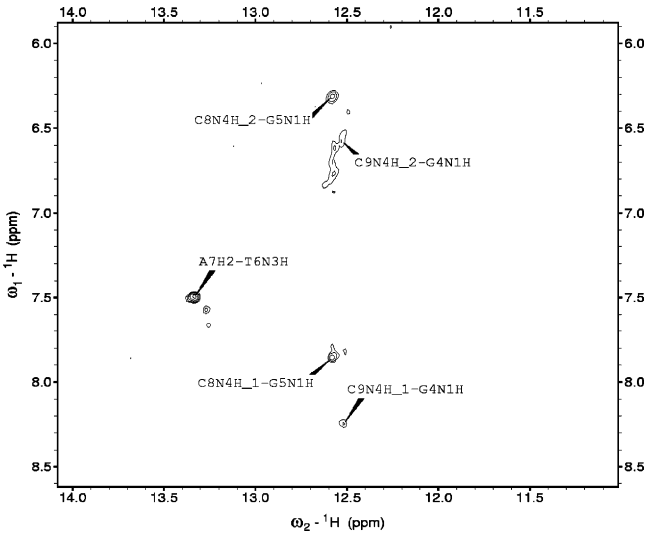

Figure 6. ^{1}H NOESY spectrum of the $[d(TATGGTACCATA)]_2/[Fe_2L_3]^{4+}$ adduct showing the imino proton region.

pair. The terminal AT base pairs are not detected because of NH exchange with bulk water at room temperature, commonly known as "fraying".

Chemical shifts of key sugar protons of oligonucleotides are known to be sensitive to conformational changes, that is, bending and twisting. However, for the helicate/DNA adduct the observed variation in chemical shifts may be induced either by conformational changes of the double-helical duplex, by being influenced by ring current effects generated by the proximity of the six bridging phenyl groups of the helicate, or by both. Thus, the proximity of the bridging phenyl groups prevents an unambiguous analysis of these shift changes in relation to sugar conformation.

Further information about the DNA structure can, in principle, be inferred from NOE distance measurements. Figure 7 shows expansions of two different regions of the NOESY spectrum recorded for **1** at 200 ms mixing time: (a) the H6/H8−H1′/H5 region and (b) the H6/H8−H2′/H2″/methyl region. To derive reliable NOE distances, the conventional approach is to record a series of NOESY spectra with progressively longer mixing times and extrapolate initial relaxation rates. In the present case, the concentration of the samples was too low to yield NOESY spectra with sufficient signal-to-noise ratio at short mixing times (<100 ms), and we were constrained to work at these low concentrations because of precipitation problems at higher concentration. However, a qualitative comparison of intra- and inter-residue NOE cross-peaks with those recorded for the native oligonucleotide shows that the T1−T6 and A7−A12 tracts represent regular B-form DNA. For the central TA residues, approximate proton−proton distances were calculated based on cross-peak intensities obtained from the 200 ms NOESY spectrum. The T6−H1′···A7−H8 distance was estimated at 5.3 Å, almost 2 Å longer than in regular B-form DNA.

An additional experiment which indicates that only the TA part undergoes conformational changes is the ^{31}P NMR spectrum shown in Figure 8. Here, the phosphorus signal assigned to the T6 3′-phosphate group is shifted 0.5 ppm upfield with respect to the native duplex, while the other phosphates experience only insignificant changes. These data indicate that each oligonucleotide strand is mainly located

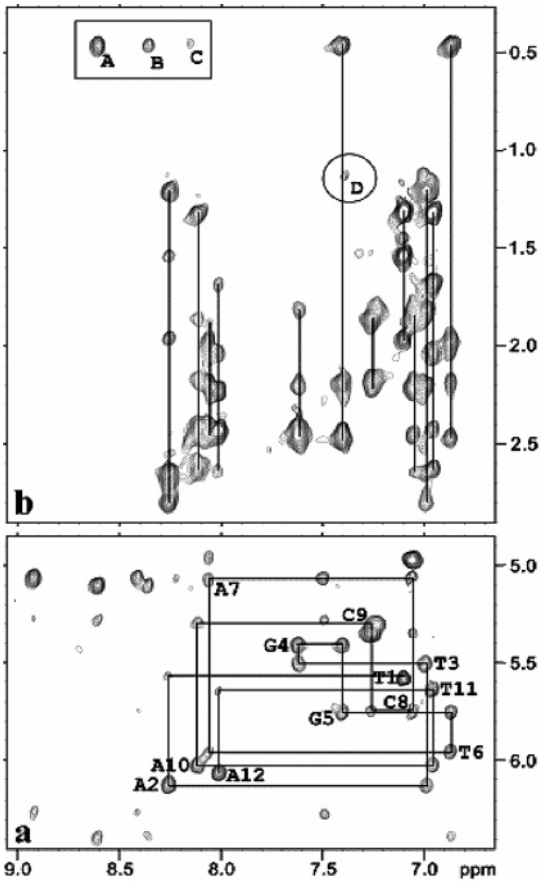

Figure 7. ^{1}H 2D NOESY spectrum of the $[d(TATGGTACCATA)]_2$/$[Fe_2L_3]^{4+}$ adduct showing the sequential pathway for the (a) H6/8−H1′/H5 region and (b) the H6/H8−H2′/2″/Methyl region. The NOESY spectrum was recorded at 293 K in D_2O using a mixing time of 200 ms. Peaks labeled A, B, and C correspond to intermolecular cross-peaks between T6-methyl and helicate H7′, −H3′, and −H4′, respectively. The peak labeled D correspond to the intranucleotide contact between T6-methyl and G5-H8 in the residual native oligonucleotide.

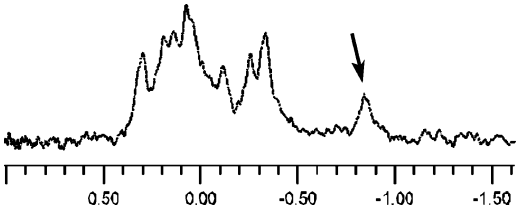

Figure 8. ^{31}P NMR spectrum of the helicate/$[d(TATGGTACCATA)]_2$ adduct.

within a typical Watson−Crick duplex structure but that there is a distortion between the central A and T residues. The distance measurements indicate that this is not a base flipping-out effect but rather a more subtle bending which moves the bases apart. Once again this is entirely consistent with what would be expected in a three-way junction structure.

The NOESY map contains surprisingly few cross-peaks corresponding to helicate−DNA proton−proton NOE contacts (d < ~5.5 Å). The main interaction is seen to involve the thymine methyl group and the pyridylimine group of the bridging ligand. Additional cross-peaks are observed between the methylene bridge protons and the sugar protons H2′/2″ of the thymine residue. NMR distances were calculated based

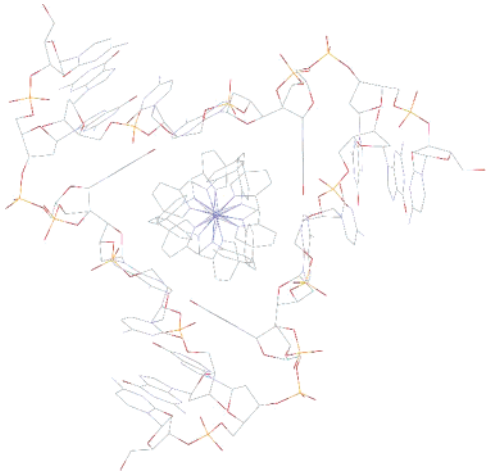

Figure 9. Three-dimensional structure of the $[Fe_2L_3]^{4+}$ - DNA complex.[1]

on a known reference distance assuming that the helicate/DNA adduct undergoes an isotropic tumbling motion, τ_C. To calculate NOE distances involving the methyl group the cross-peaks were scaled to the intra-thymine Me5···H6 cross-peak intensity. The fast spinning methyl protons are represented by a pseudoatom located at the center of the triangle formed by the three protons. Calculations based on thymine proton crystal coordinates gives a pseudoatom···H6 distance of 3.1 Å which was used as reference.[20] The NOESY cross-peak pattern for adduct **2** is, within experimental errors, practically identical to that of adduct **1**.

Comparison between the NMR and the X-ray Structure of 2. The X-ray structure of the DNA supramolecular structure of **2** is shown in Figure 9. The 3WJ is formed by three strands of the sequence 5′-(CGTACG) and forms a central trigonal hydrophobic cavity. The phenyl rings at the center of the helicate form extensive π-stacking interactions with the thymine and adenine bases at the junction. In this arrangement one phenyl ring in the bridge is stacked on thymine T3, whereas the second phenyl ring is stacked on adenine A4. Because of the 3-fold symmetry of the helicate which matches the 3-fold junction, this double stacking interaction is repeated 3 times.

The strong ring current effects induced by extensive π-stacking produce large upfield chemical shifts for the aromatic protons of the bridging phenyl rings (see Table 3). To make a detailed comparison of proton−proton distances of the X-ray and NMR structures, the relevant hydrogen coordinates had to be added to the carbon atoms on the basis of appropriate hybridization since the positions of the hydrogen atoms were not determined in the crystal structure. With consideration of the relatively large error limits in NOE distances and the fact that the solution structure is expected to be more flexible and relaxed than that in the crystal, the agreement between the NMR and X-ray structures is seen to be satisfactory (Table 4).

One additional observation in support of the close resemblance between solid state and solution structure may be mentioned. In the H6/H8−H2′/2″ NOESY region (Figure

(20) Nerdal, W.; Hare, D. R.; Reid, B. R. *J. Mol. Biol.* **2001**, 717−739.

Table 4. List of Key Intermolecular Proton−Proton Distances from the NMR and X-ray Analysis, Respectively

distances (Å)	NMR	X-ray
T3-Me(ps)···H3	4.4	5.2
T3-Me(ps)···H4	5.2	7.5
T3-Me(ps)···H7	3.9	3.6
T3-Me(ps)···H10	4.3	4.3
T3-Me(ps)···H11	4.4	4.7

[a] Hydrogen coordinates are added based on the X-ray data. Distances involving the methyl group are calculated assuming a pseudoatom for the methyl protons.

7), one may notice that the T6−H2′/2″ protons have almost identical chemical shifts which can only be explained by invoking rapid endo/exo motion of the sugar atom T6−C2′. This observation is in perfect agreement with the 3WJ crystal structure where the electron density map shows no density above the noise level at this particular site because of conformational disorder (private communication).

In summary, the NMR data establish the following experimental facts: (i) the stoichiometry of the adduct for both **1** and **2** is consistent with a 1:3 ratio between helicate and single strand; (ii) the 2-fold symmetry of the helicate is lifted, but the 3-fold symmetry is retained; (iii) significant chemical shift differences and NOE contacts are only observed for the central TA step in the duplex; (iv) the aromatic protons of the bridging ligands experiences dramatic chemical shifts consistent with large ring current perturbations. Since a potential groove binding would give rise to several NOE contacts and most importantly, lift the 3-fold symmetry, the only structure compatible with the above observation is a three-way junction with the helicate in the center.

DNA junctions are unique structures that consist of several double strands converging at one point. Three-way junctions (3WJs) consisting of three double arms connected at the junction point are the simplest and most commonly occurring branched nucleic acids. In RNA, they are involved in crucial biological functions such as splicing[21] and translation.[22] In DNA, 3WJs are formed transiently during DNA replication (the replication fork).[23] They are intermediate structures during triplet repeat expansions,[15a] anomalies associated with several human genetic diseases such as myotonic dystrophy type 1 and Huntington's disease.[15b] 3WJs are present in the inverted terminal repeats of certain viral genomes[15c] and are intermediate during phage genetic recombination.[15e]

3WJs form flexible Y-shaped structures in the presence of metal ions such as Mg^{2+}. Previously, a NMR structure of a 3WJ model has been reported where stoichiometric samples of three non-palindromic strands (two 10-mers and one 12-mer) were assembled in the presence of $MgCl_2$.[24] One of the three arms contains two extra-helical residues which tend to destabilize a normal duplex and consequently promote the formation of 3WJ. The transformation of a regular, stable palindromic duplex to a 3WJ has to our knowledge never been reported to take place in solution.

Conclusions

We have presented a detailed NMR analysis of the interaction between a binuclear iron(II) supramolecular helicate, $[Fe_2L_3]^{4+}$, and two double helical oligodeoxyribonucleotides. The composition of the adducts corresponds to a 1:3 helicate/ssDNA ratio. The 2-fold symmetry of the helicate is lifted while the 3-fold symmetry is retained. The NOE contacts between the helicate and DNA are compatible with a binding pattern where the helicate is positioned in a trigonal symmetric environment. The bridging phenyl rings experience extreme chemical proton shifts induced by close π-stacking with the central nucleobases. The NMR solution data are in substantial agreement with the recently published crystal structure of an adduct formed between the helicate and **2** where the helicate is situated in the center of a three-way junction. It is not unusual that molecular arrangement of very high symmetry is preferred in crystallographic environment because of low crystal-packing energy. Thus, it is remarkable that the high-symmetric trigonal form of the three-way junction is retained in solution. Previously, 3WJ constructs have been engineered by introducing bulges, mismatched, or both into the complementary sequences. This is the first time a regular palindromic duplex has been shown to form a 3WJ. A regular non-palindromic duplex does not have the ability to form the same type of 3WJ. The key feature in biomolecular DNA recognition motifs is the size and shape of the molecular surface which matches to the size and shape of the DNA target and provide a variety of recognition points. One may envision that the three-way DNA junction structure is an appropriate target for design of a new family of ligands with a high structural specificity and strong binding characteristics.

Acknowledgment. This work was supported by the MARCY Research Training Network (EU-Contract CT-2002-00175), COST Action D20, WG 0010/02, and The Norwegian Research Council (Project-148992/V40).

Note Added after ASAP Publication. This article was released ASAP on April 4, 2007, with incorrect artwork for Figure 8. The correct version was posted on April 19, 2007.

IC062415C

(21) Guthrie, C.; Patterson, B. *Annu. Rev. Genet*. **1988**, *22*, 387−419.

(22) Nikulin, A.; Sarganov, A.; Ennifar, E.; Tishchenk, S.; Nevskaya, N.; Shepard, W.; Portier, C.; Garber, M.; Ehresmann, B.; Ehresmann, C.; Nikonov, S.; Dumas, P. *Nat. Struct. Biol.* **2000**, *7*, 273−277.

(23) Singleton, M. R.; Scaife, S.; Wigley, D. B. *Cell* **2001**, *107*, 79−89.

(24) Thiviyanathan, V.; Luxon, B. A.; Leontis, N. B.; Illamgasekaree, Donne, D. G.; Gorenstein, D. G. *J. Biomol. NMR* **1999**, *14*, 209−221.